Efficiency Studies and PID Cut Optimization for E08-027

Melissa Cummings
The College of William and Mary
melissac@jlab.org

June 10th, 2013

Abstract

The g_2^p experiment requires good particle identification to minimize pion contamination in the asymmetries and cross sections. To achieve this, a combination of a gas Cherenkov detector and lead glass electromagnetic calorimeter was used on each arm of the High Resolution Spectrometers. This document will discuss the procedure and results of an efficiency study completed for the gas Cherenkov and lead glass calorimeters. An optimization of the particle ID cuts was performed to minimize pion contamination, taking into account the cut efficiences.

1 Introduction

In order to distinguish between electrons and pions, a gas Cherenkov detector is used in conjunction with an electromagnetic lead glass calorimeter in each of the High Resolution Spectrometers. The gas Cherenkov is a threshold detector designed such that lighter particles (electrons) will emit Cherenkov radiation when passing through the CO_2 gas, wheras a heavier particle (such as a pion) will not. Energetic particles that pass through the lead glass will produce a cascade of secondary particles. As this "shower" of particles propogates through the medium, the particle's energy is converted to light, which is then collected and used to determine the initial energy of the particle.

2 Right HRS

2.1 Detector Layout

The first layer of the calorimeter on the RHRS, the preshower, is composed of forty-eight lead glass blocks, oriented perpendicular to the particle track. Each block is 10 cm x 10 cm x 35 cm. The second layer, the shower, is composed of eighty blocks, which are oriented parallel to the particle track. Each block is 15 cm x 15 cm x 35 cm.

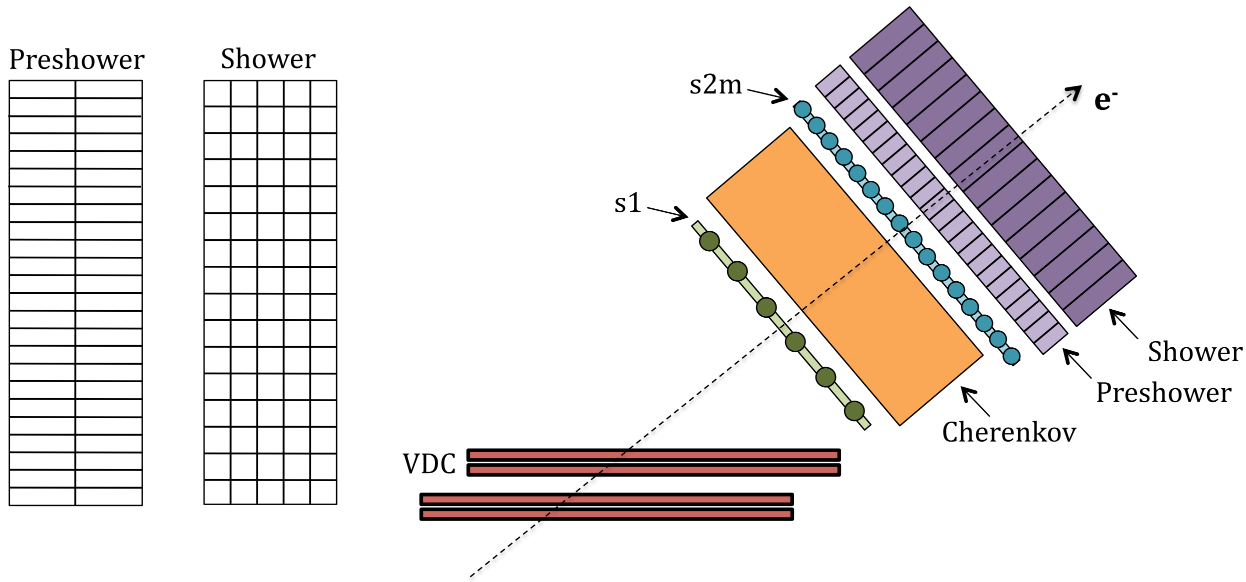

Figure 1: Face view of the preshower/shower detectors and a side view of the RHRS detector stack.

2.2 Selection of Good Electrons

Initial cuts were made on the golden track variables θ, ϕ and dp to get rid of events on the edge of the acceptance. Additionally, a cut was made to require only single track events. These cuts can be seen for the RHRS in Figure 2, and are applied for all efficiency studies described below.

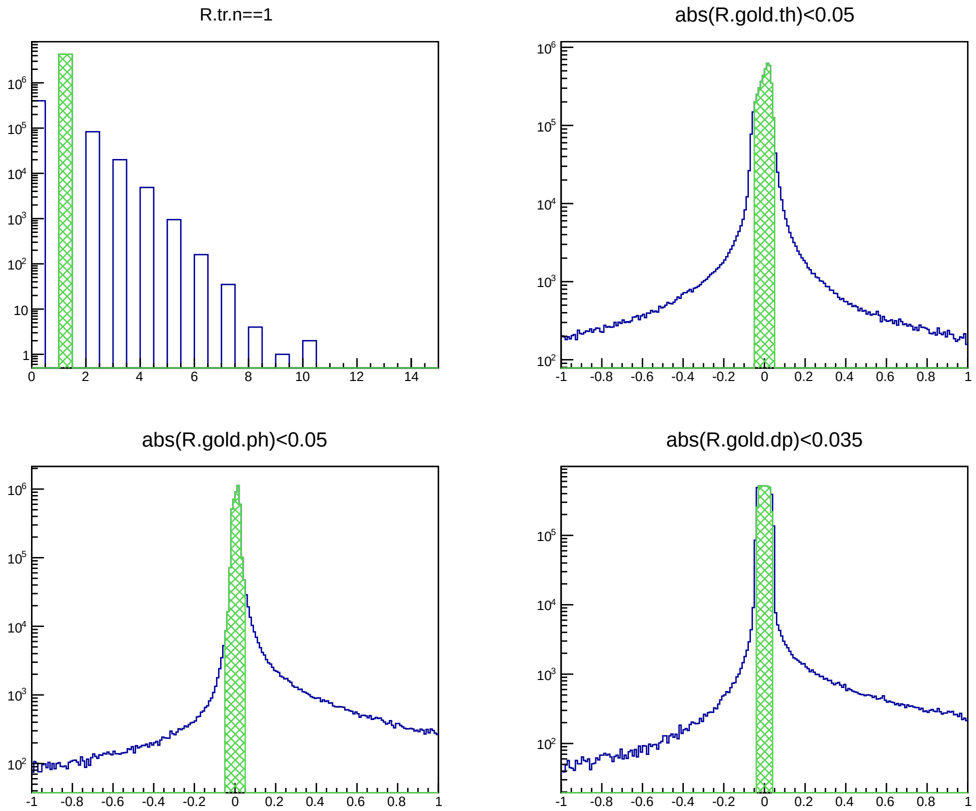

Figure 2: Cuts to select good events for the RHRS. The blue line represents the raw variable, while the shaded region indicates the selected events.

2.3 Detector Efficiences

The detection efficiency is an indicator of the performance of the detector throughout the run period. To determine the detector efficiency for the preshower/shower detectors, a selection of electrons that triggered the gas Cherenkov (and fell well above the single-photoelectron peak threshold) is made. The number of these events that *also* trigger the preshower and shower are then counted.

$$num_{cer} = \#\text{ of events selected in Cherenkov}$$

$$num_{pr} = \#\text{ of events also detected in Lead Glass}$$

$$\text{efficiency} = \frac{num_{pr}}{num_{cer}}$$

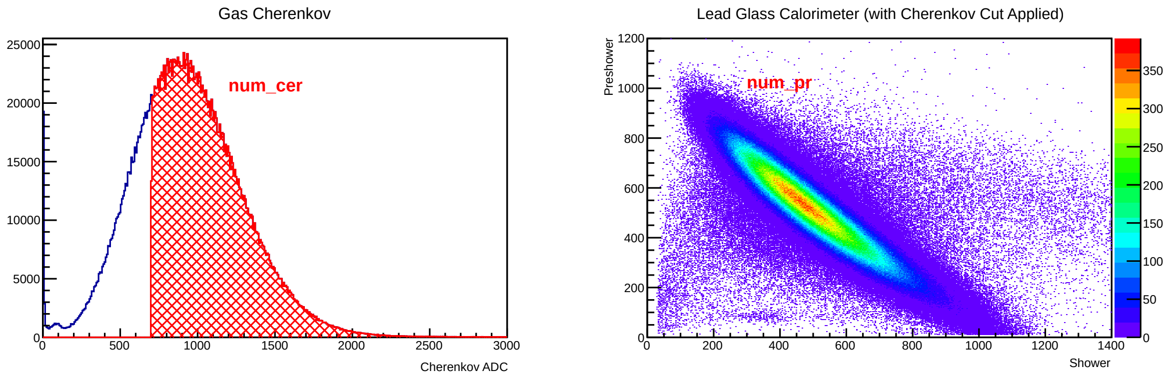

Figure 3: The plot on the left shows the selection of events that triggered the gas Cherenkov.

The detector efficiency for the preshower/shower was found to be very high (above 98.8%) for all kinematic settings (figure 4).

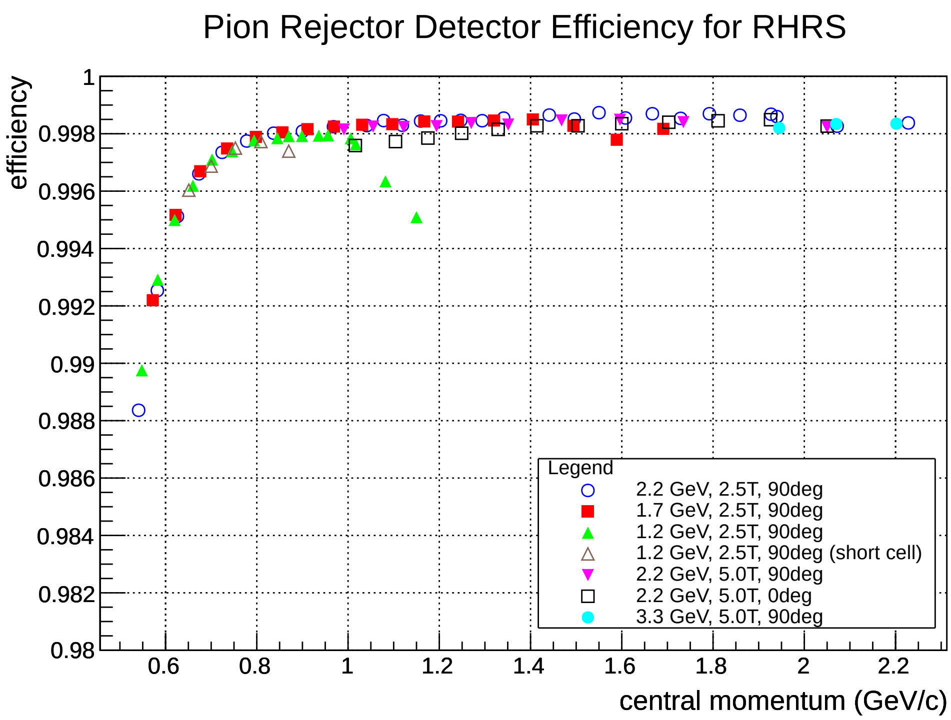

Figure 4: Detector efficiencies for the RHRS lead glass calorimeters.

Similary, the detection efficiency of the gas Cherenkov is determined by selecting a sample of events that were seen in the lead-glass calorimeter, and counting the number of these events that *also* fired the gas Cherenkov.

$$num_{pr} = \#\text{ of events selected in Preshower/Shower}$$

$$num_{cer} = \#\text{ of events also detected in gas Cherenkov}$$

$$\text{efficiency} = \frac{num_{cer}}{num_{pr}}$$

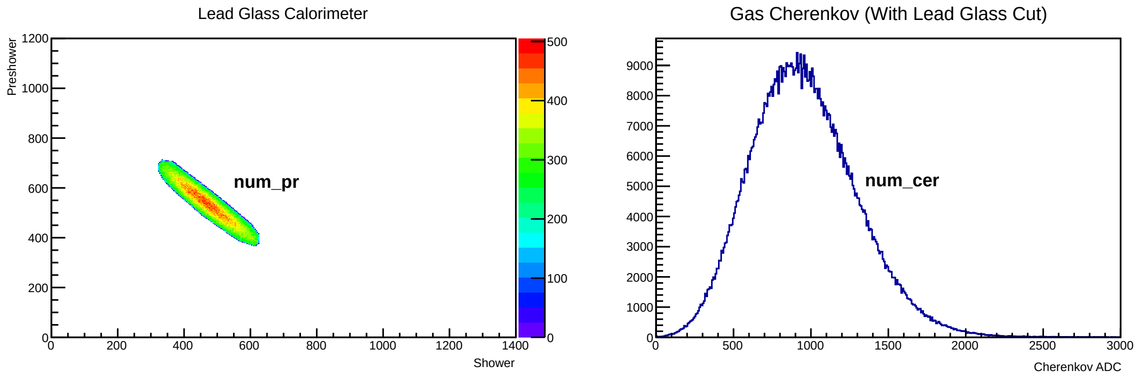

Figure 5: Selection of events that triggered the gas Cherenkov.

Again, the detection efficiency was found to be very high (above 99.8%) across the entire range of kinematics (figure 6).

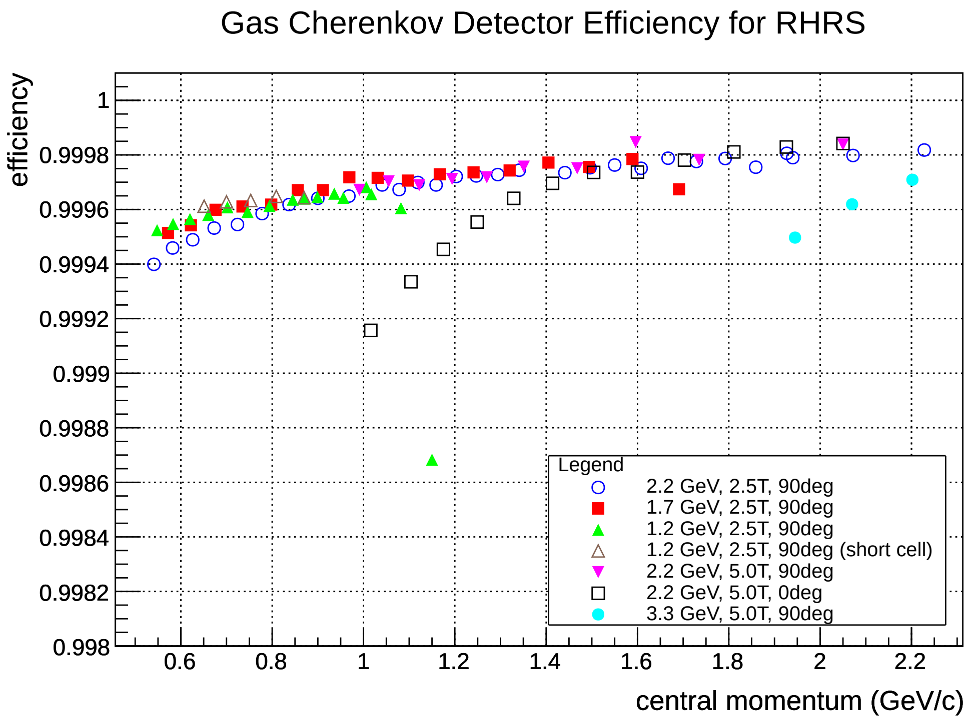

Figure 6: Detector efficiences for the RHRS gas Cherenkov.

2.4 Cut Efficiences

There are three cuts used for particle identification; a gas Cherenkov threshold cut, a cut on the first layer of lead glass (preshower/p), and a cut on the total energy deposited in the calorimeter divided by the particle's momentum (E/p). These cuts are chosen to maximize pion supression while minimizing the inefficiency caused by cutting out good electron events. On the RHRS, the gas Cherenkov cut was placed at channel 150, which maintains a high electron detection efficiency (greater than 99.5%) for all but one kinematic settings. The one exception has a detection efficiency greater then 98.7%, as seen in figure 7.

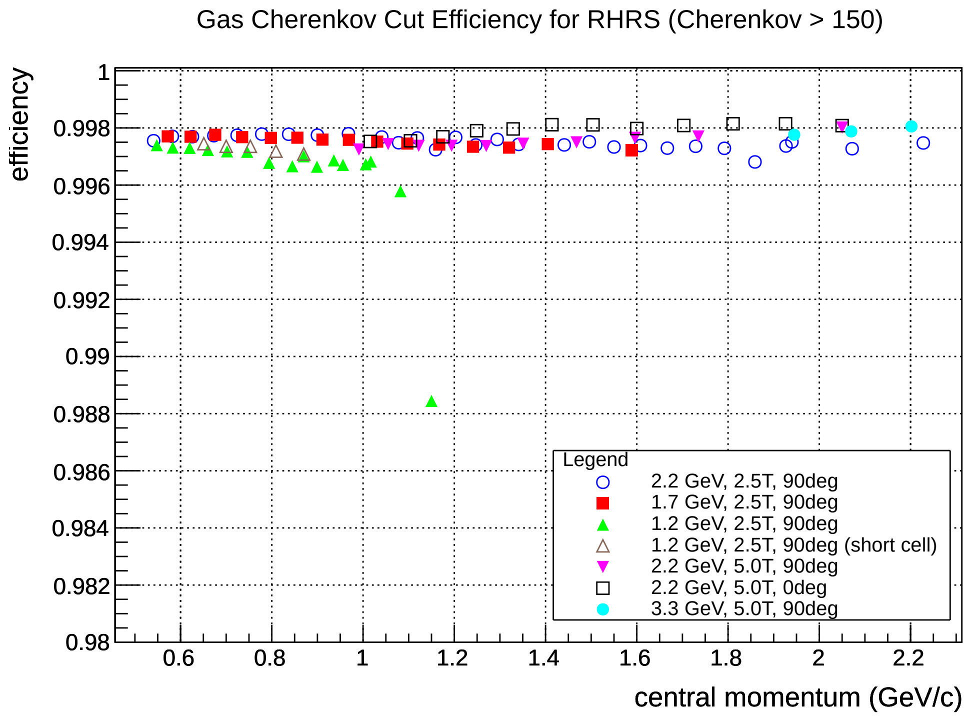

Figure 7: Cut efficiency for the RHRS gas Cherenkov.

The lead glass cuts are chosen such that the overall electron detection efficiency does not fall below 99%. Different to the gas Cherenkov, the cuts on the calorimeter are momentum dependent, and so were determined seperately for each kinematic setting. A conservative cut is placed on the preshower, and a seperate cut is placed on the summed energy in both layers. The plots below show the trend of these cuts over the full range of kinematic settings. For some of the kimematic settings during the 1.2 GeV energy setting, a short ammonia cell was used. Seperate cuts were made for these runs.

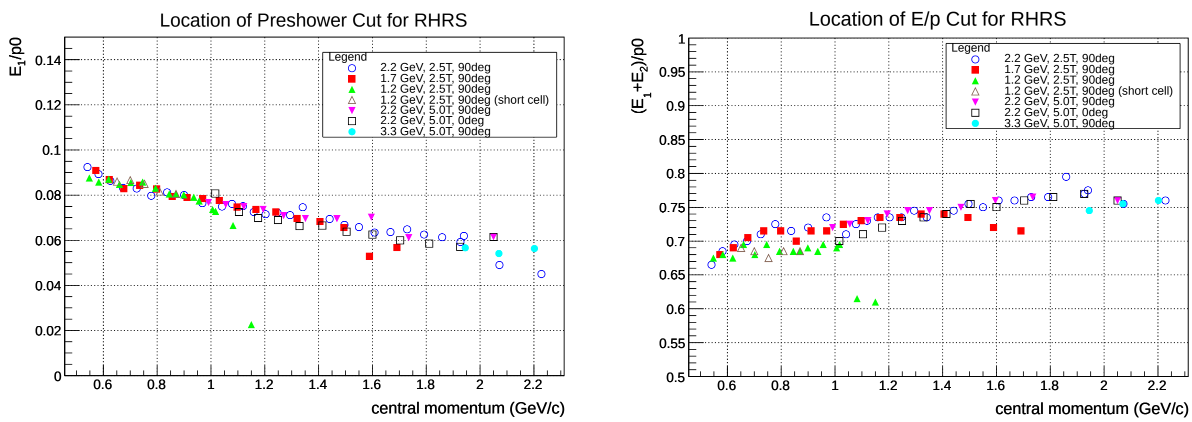

Figure 8: Trend of cuts on lead glass for RHRS versus central momentum.

The cut efficiency for the preshower/shower is approximately 99% for all kinematic settings, as can be seen in figure 9.

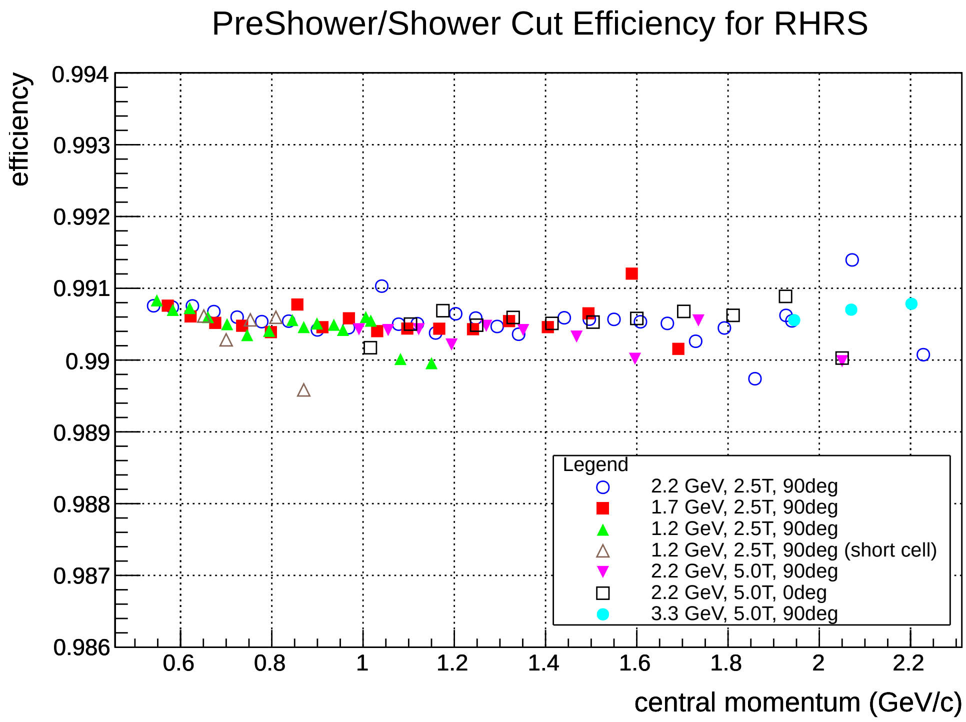

Figure 9: Cut efficiency for the RHRS lead glass calorimeters

2.5 Pion Suppression

The overall pion supression can be examined by applying the three cuts described above and looking at the level of pion contamination that remains. We can see the effect of the gas Cherenkov and preshower cuts on the overall pion suppression in figure 10. The cut on the Cherenkov removes most of the contamination, while the preshower cut removes events at lower energy.

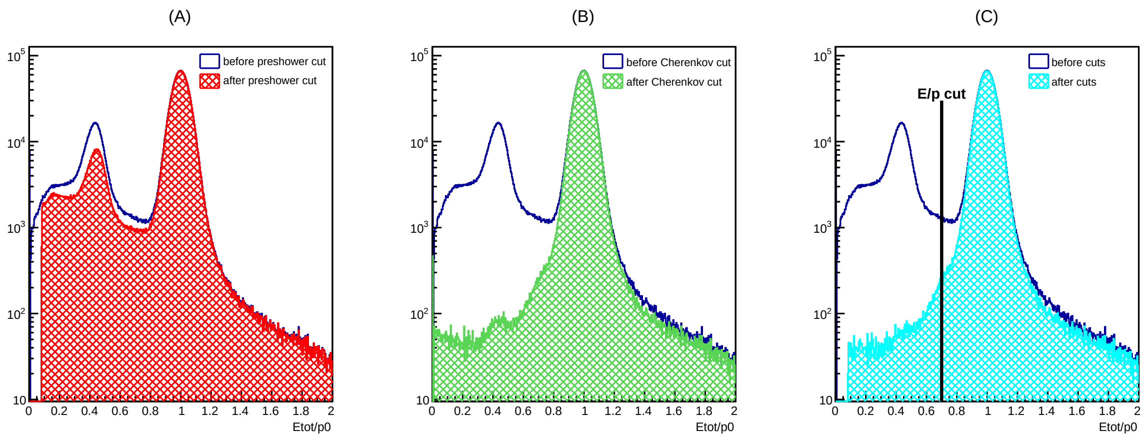

Figure 10: This set of plots shows the E/p distribution; the total energy deposited in the calorimeter divided by the particle's momentum. (A) shows the effect of a cut on the preshower while (B) shows the effect of the gas Cherenkov cut. (C) shows the result of applying both cuts, with the black line indicating the location of the E/p cut.

The level of pion contamination, before any cuts are applied, can be seen in figures ?? and ??. The level of residual pion contamination is very low, with $\pi/e < 0.0052$ for all kinematic settings, as seen in figure 12.

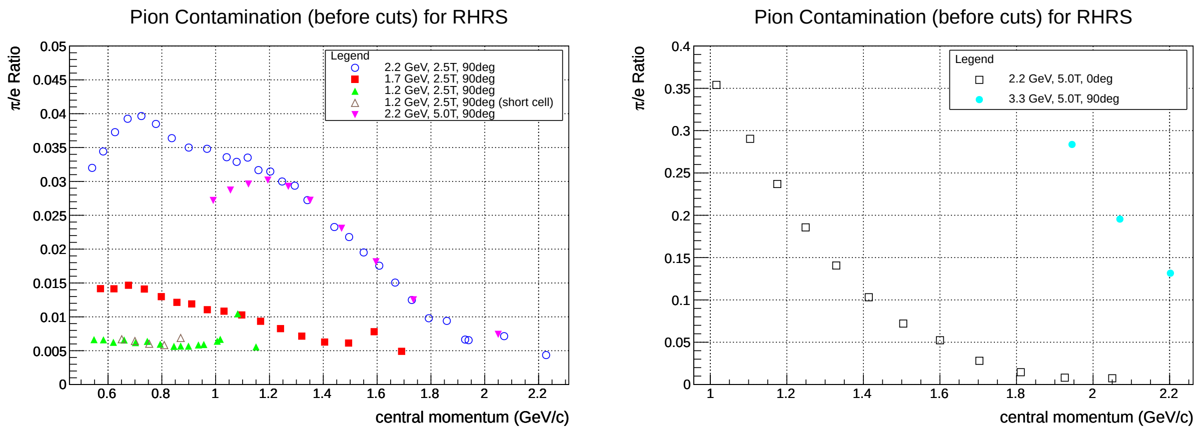

Figure 11: Trend of cuts on lead glass for RHRS versus central momentum.

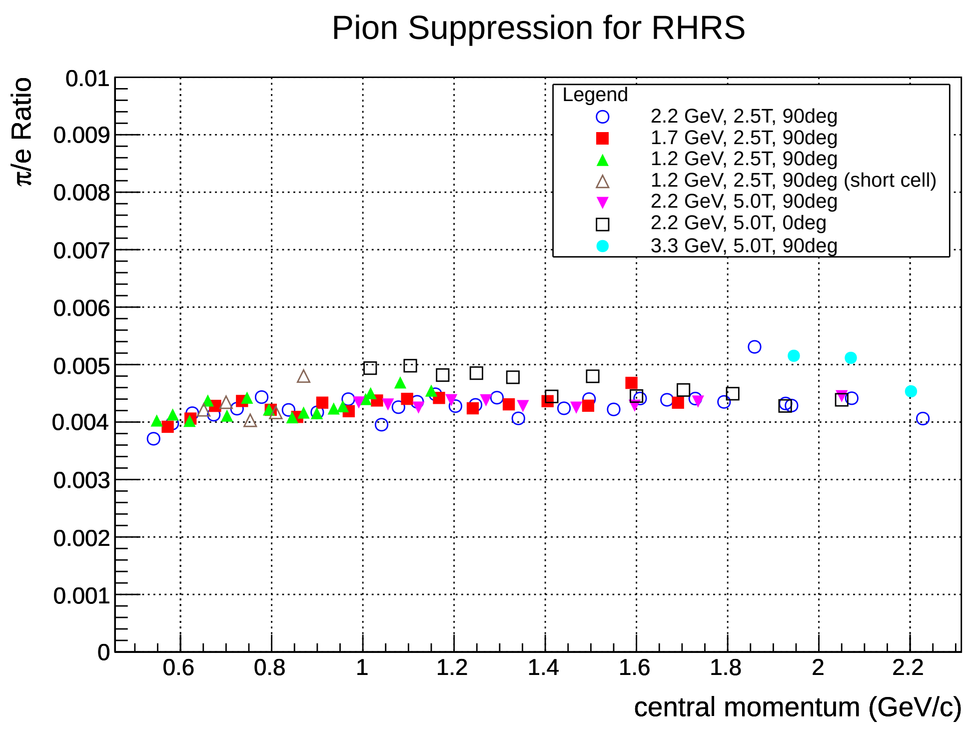

Figure 12: Residual pion contamination for the RHRS.

3 Left HRS

3.1 Detector Layout

The lead glass calorimeter on the LHRS differs from the RHRS in that it is not a total energy absorption detector. Both layers are made up of thirty-four lead glass blocks, oriented perpendicular to the particle track. The blocks that make up the first layer are 15 cm x 15 cm x 30 cm, while the blocks that make up the second layer are 15 cm x 15 cm x 35 cm.

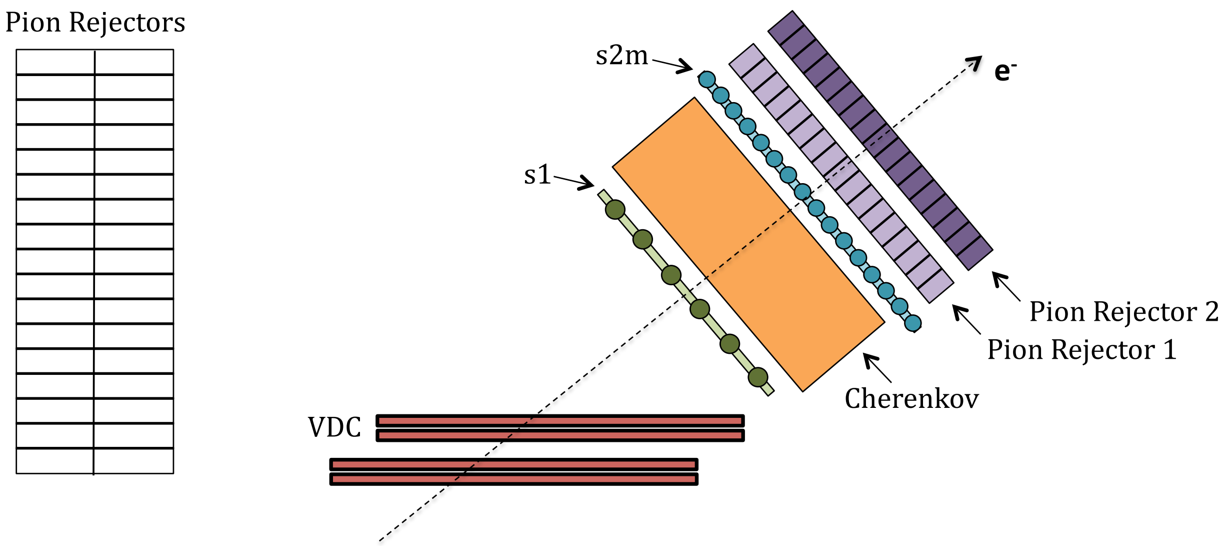

Figure 13: On the left is a face view of the pion rejector layers. On the right is a diagram of the LHRS detector stack.

3.2 Selection of Good Electrons

Cuts were made initally on the golden varibales θ, ϕ and dp to get rid of events on the edge of the acceptance. Additionally, a cut was made to require only single track events. Figure 14 shows these cuts for the LHRS. Again, these cuts are applied for all efficiency studies described below.

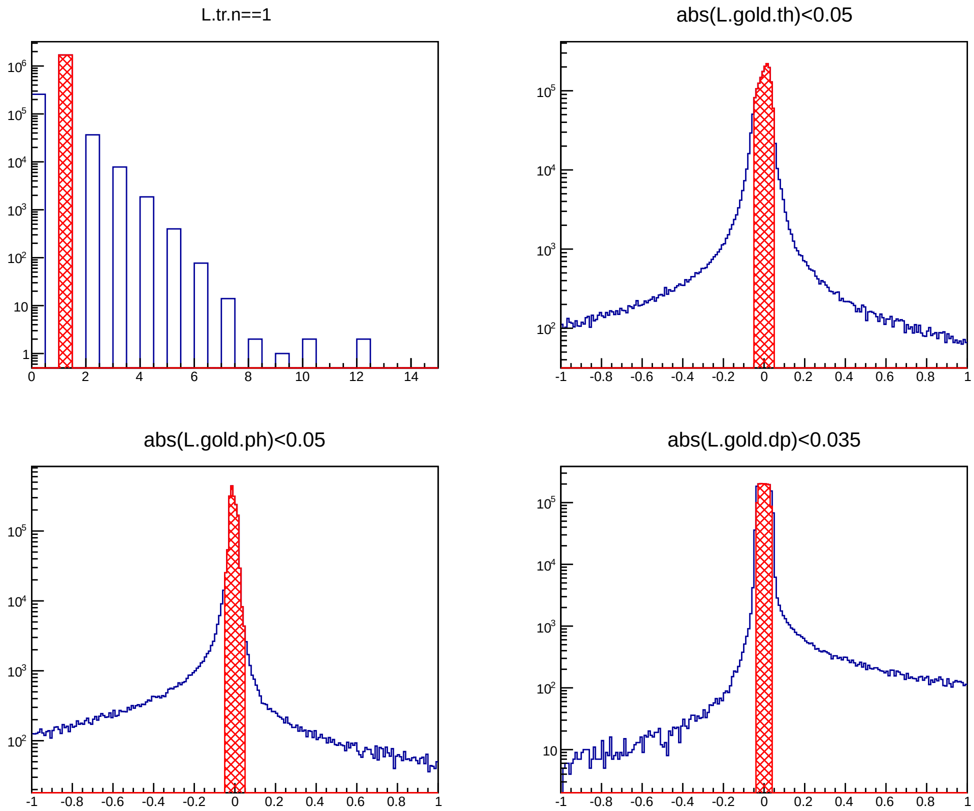

Figure 14: Cuts made to select good events for the LHRS. The blue line represents the raw variable while the shaded region shows the events selected by the cut.

3.3 Detector Efficiences

Similar to the RHRS, detection efficiences were determined for the LHRS to test the performance of the detectors throughout the run period. For the gas Cherenkov, the detector efficiency is determined by selecting events in the pion rejectors and then counting the number of these events that *also* trigger the Cherenkov. The efficiency of the LHRS gas Cherenkov was found to be very high (above 99.8%) for all kinematic settings.

Similarly, the detection effiency of the pion rejectors is determined by selecting a sample of events in the gas Cherenkov, and counting the number of events in this sample that also trigger *both* layers of the lead-glass. For the LHRS, it was necessary to adjust this procedure slightly. It was found that the detection efficiency dopped considerably for momentum settings lower than 0.9 GeV/c. The problem, however, appears to not be an actual inefficiency of the system, but rather a consequence of the design of the detector. As was described above, the layers of lead-glass on the LHRS are identical, compared to the RHRS where the shower layer is considerably thicker than the preshower layer. For low momentum settings, some electrons deposit the majority of their energy in the first layer of lead-glass, therefore not firing the second layer. To account for this, a seperate condition was created for these low momentum settings. An event would still be counted even if it had no hit in the second layer, as long as the majority (that is $E \geq E_{tot} - 30$ MeV) of the total energy had been deposited in the first layer. As can be seen in figure 16, the detection efficiency for the lead-glass is above 98% for all kinematic settings with this new condition.

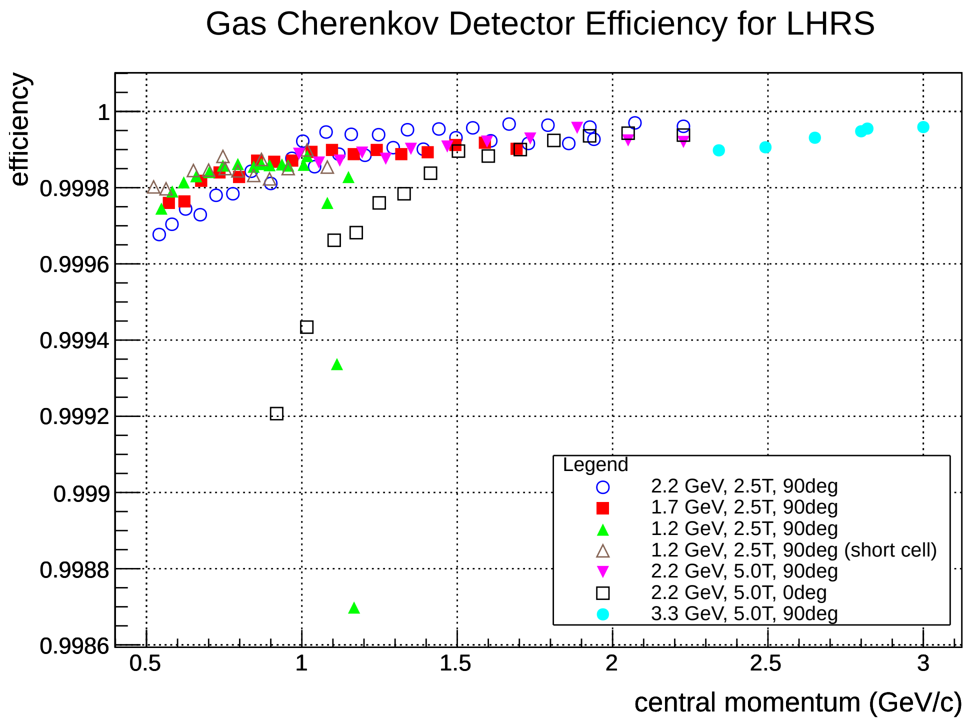

Figure 15: Gas Cherenkov detector efficiency for the LHRS

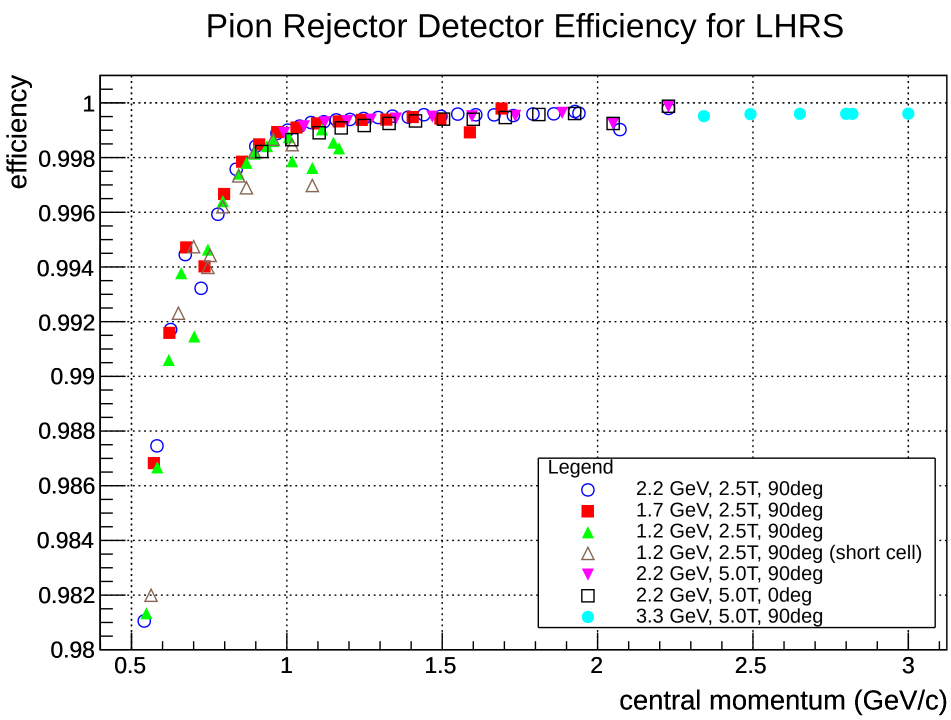

Figure 16: Pion rejector detector efficiencies for the LHRS

3.4 Cut Efficiencies

Similar to the RHRS, there are three cuts used for particle identifcation; a gas Cherenkov threshold cut, a cut on the first layer of the lead-glass detector (layer1/p), and an E/p cut. These cuts are made to maximize pion supression while minimizing the inefficiency caused by cutting out good electron events. For the LHRS gas Cherenkov, the cut was placed at channel 200. The cut efficiency displayed in the plot below shows that the electron detection efficiency is very high (greater than 99.8%) for all kinematic settings.

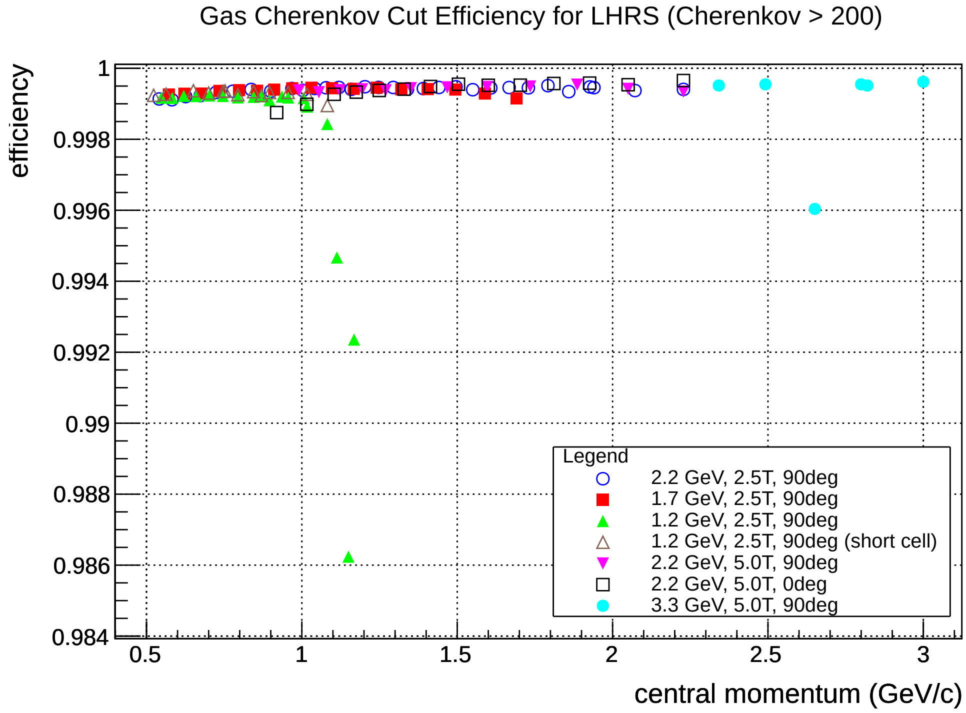

Figure 17: Cut Efficiency for the LHRS gas Cherenkov

The lead glass cuts are chosen such that the electron detection efficiency does not fall below 99%. Since these cuts on the pion rejectors are momentum dependent, they were determined seperately for each kinematic setting. In comparison to the RHRS, the cut on the first layer of the lead glass does not need to be as conservative, since more energy is deposited in the layer one of the pion rejector than the (thinner) preshower. The figure below shows the trend of these cuts over all kinematic settings.

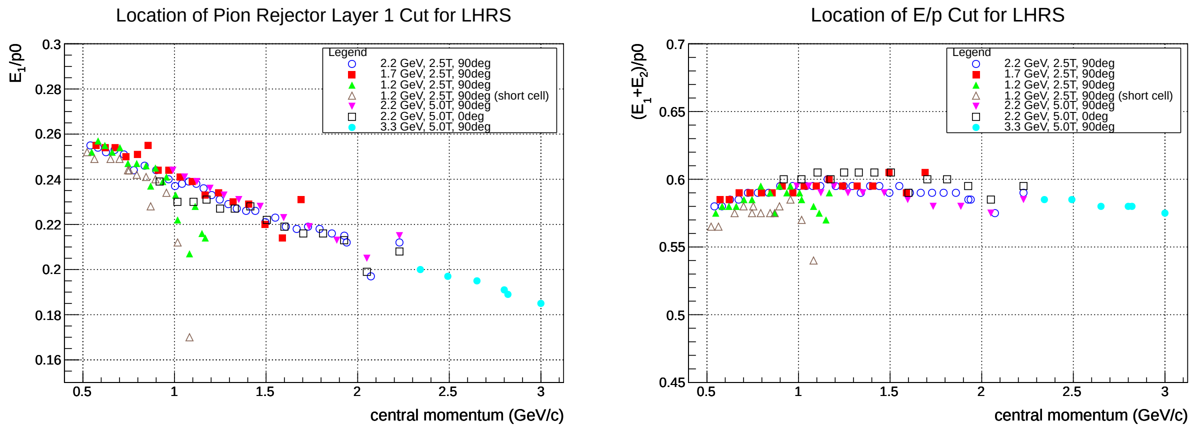

Figure 18: Trend of cuts on lead-glass for LHRS

The cut efficiency for the pion rejectors is approximately 99% for all kinematic settings, as can be seen in figure 19.

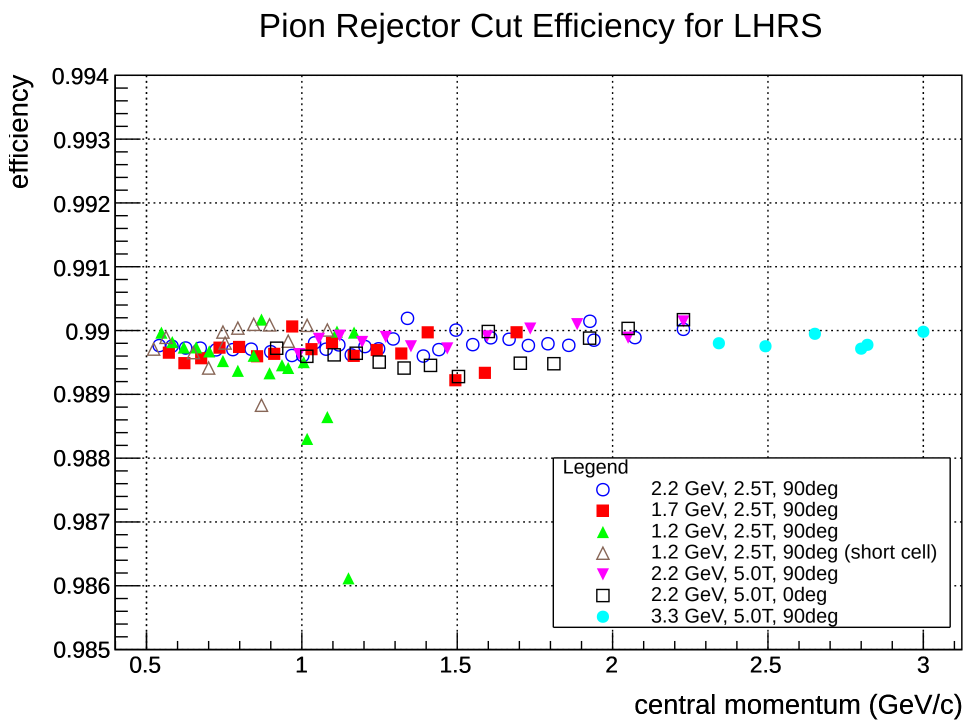

Figure 19: Cut efficiency for the LHRS lead glass calorimeters

3.5 Pion Supression

Again, the overall pion suppression can be examined by looking at the remaining pion contamination after applying the above cuts. Figure 20 shows the effects of these cuts.

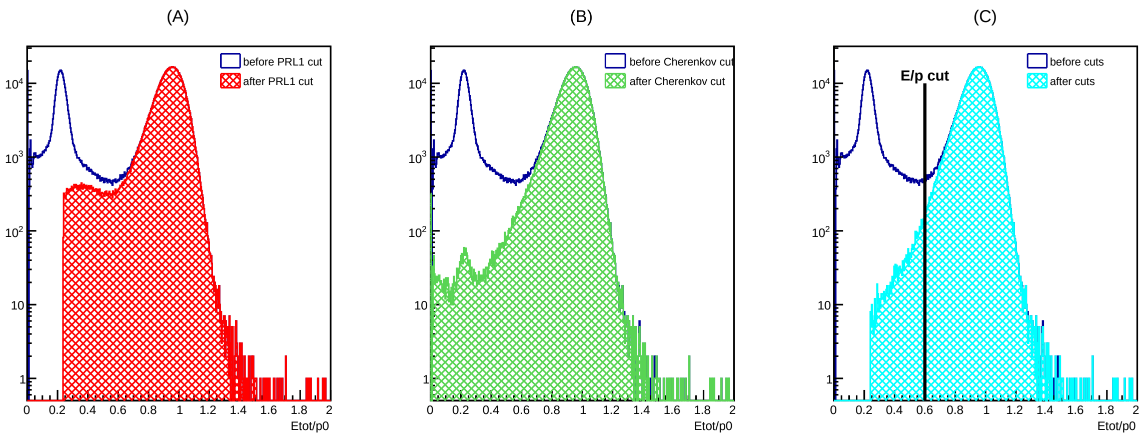

Figure 20: This set of plots shows the E/p distribution; the total energy deposited in the calorimeter divided by the particle's momentum. (A) shows the effect of a cut on the first layer of the pion rejector while (B) shows the effect of the gas Cherenkov cut. (C) shows the result of applying both cuts, with the black line indicating the location of the E/p cut.

The level of residual pion contamination is very low, with $\pi/e < 0.0045$ for all kinematic settings (with one exception), as seen in figure 22.

The level of pion contamination, before any cuts are applied, can be seen in figures **??** and **??**. The level of residual pion contamination is very low, with $\pi/e < 0.0052$ for all kinematic settings, as seen in figure 22.

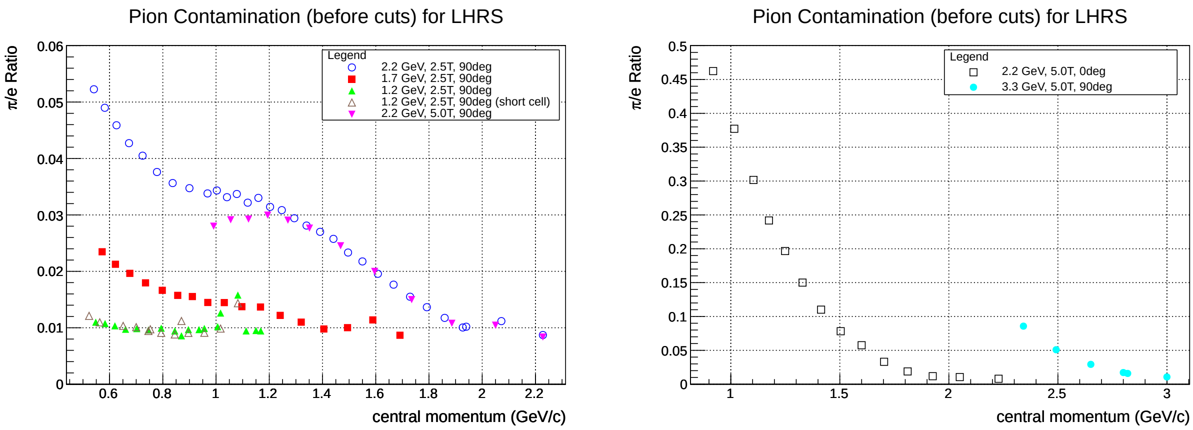

Figure 21: Trend of cuts on lead glass for RHRS versus central momentum.

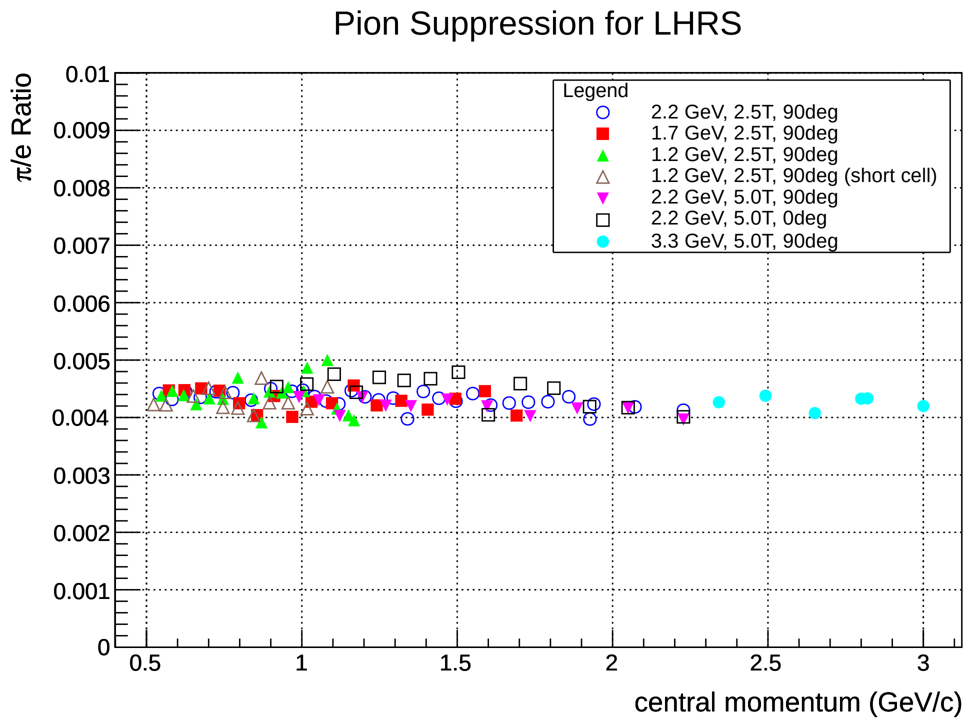

Figure 22: Residual pion contamination over all kinematic settings

4 Conclusion

Detection efficiences were found to be high over the entire range of kinematics, indicating good detector performance throughout the run period. The pion rejector effiency (LHRS) was seen to drop for runs lower than 0.9 GeV/c, due to the physical properties of the detector. Particle identification cuts were determined to maintain an overall electron detection efficiency of 99%. The residual pion contamination was found to be very low for both the left and right HRS over the full range of kinematic settings.

5 Data Tables

Contained in the following tables is the results of this analysis. The table entries are described below:

Det Eff (Cer): detector efficiency of the gas Cherenkov (Cer) or lead glass calorimeter (PR)
Cut on pr1/p0: location of cut on the first layer of lead glass

- Det Eff: detector efficiency of the gas Cherenkov (Cer) or lead glass calorimeter (PR)
- $(\pi/e)_{raw}$: the initial π/e ratio (without cuts)
- Cut on E_1/p0: location of cut on the first layer of lead glass
- Cut on E_{tot}/p0: location of cut on the total energy deposited in the lead glass
- Cut Eff: cut efficiency of the gas Cherenkov (Cer) or lead glass calorimeter (PR) cuts
- $(\pi/e)_{final}$: the final π/e ratio (with all cuts)

5.1 Right HRS Results

Note that for all kinematic settings, the cut on the gas Cherenkov is at channel 150.

Table 1: RHRS, E = 2.2 GeV, 2.5T 90 deg Target Field

p0 (GeV/c)	Run #	Det Eff (Cer)	Det Eff (PR)	$(\pi/e)_{raw}$	Cut on E_1/p0	Cut on E_{tot}/p0	Cut Eff (PR)	Cut Eff (PR)	$(\pi/e)_{final}$
0.541	22969	0.99940	0.98836	0.03200	0.0924	0.665	0.99076	0.99755	0.00371
0.582	22962	0.99946	0.99254	0.03442	0.0893	0.685	0.99074	0.99771	0.00397
0.626	22955	0.99949	0.99512	0.03727	0.0863	0.695	0.99075	0.99769	0.00415
0.673	22947	0.99953	0.99660	0.03925	0.0832	0.700	0.99068	0.99773	0.00413
0.724	22941	0.99955	0.99735	0.03965	0.0829	0.710	0.99060	0.99774	0.00423
0.778	22932	0.99959	0.99775	0.03849	0.0797	0.725	0.99054	0.99778	0.00443
0.837	22925	0.99962	0.99802	0.03639	0.0812	0.715	0.99054	0.99778	0.00421
0.900	22919	0.99964	0.99809	0.03500	0.0800	0.720	0.99042	0.99775	0.00417
0.968	22913	0.99965	0.99825	0.03482	0.0764	0.735	0.99045	0.99780	0.00440
1.041	22904	0.99969	0.99828	0.03357	0.0749	0.710	0.99103	0.99768	0.00395
1.078	22653	0.99967	0.99846	0.03289	0.0761	0.725	0.99050	0.99748	0.00426
1.119	22893	0.99970	0.99830	0.03352	0.0751	0.730	0.99051	0.99765	0.00435
1.159	22641	0.99969	0.99844	0.03167	0.0725	0.735	0.99038	0.99724	0.00448
1.203	22875	0.99972	0.99845	0.03147	0.0715	0.735	0.99065	0.99767	0.00428
1.247	22625	0.99972	0.99847	0.02999	0.0722	0.735	0.99059	0.99740	0.00430
1.294	22862	0.99973	0.99845	0.02937	0.0711	0.745	0.99047	0.99760	0.00442
1.341	22607	0.99974	0.99855	0.02724	0.0746	0.735	0.99036	0.99742	0.00406
1.441	22585	0.99974	0.99865	0.02326	0.0694	0.745	0.99059	0.99741	0.00424
1.496	22831	0.99975	0.99851	0.02178	0.0668	0.755	0.99057	0.99752	0.00440
1.550	22564	0.99976	0.99873	0.01951	0.0658	0.750	0.99057	0.99733	0.00422
1.608	22816	0.99975	0.99855	0.01755	0.0634	0.760	0.99053	0.99738	0.00441
1.667	22551	0.99979	0.99870	0.01506	0.0636	0.760	0.99051	0.99729	0.00439
1.729	22798	0.99978	0.99854	0.01249	0.0648	0.765	0.99026	0.99736	0.00441
1.792	22529	0.99979	0.99870	0.00979	0.0625	0.765	0.99045	0.99729	0.00435
1.859	22786	0.99976	0.99865	0.00940	0.0613	0.795	0.98974	0.99681	0.00531
1.927	22513	0.99981	0.99868	0.00664	0.0592	0.770	0.99062	0.99737	0.00432
1.940	22977	0.99979	0.99860	0.00655	0.0619	0.775	0.99055	0.99751	0.00429
2.072	22493	0.99980	0.99826	0.00715	0.049	0.755	0.99140	0.99727	0.00441
2.228	22363	0.99982	0.99838	0.00436	0.045	0.760	0.99008	0.99747	0.00406

Table 2: RHRS, E = 1.7 GeV, 2.5T 90 deg Target Field

p0 (GeV/c)	Run #	Det Eff (Cer)	Det Eff (PR)	$(\pi/e)_{raw}$	Cut on E_1/p0	Cut on E_{tot}/p0	Cut Eff (PR)	Cut Eff (PR)	$(\pi/e)_{final}$
0.572	23500	0.99951	0.99220	0.01416	0.0909	0.680	0.99076	0.99771	0.00392
0.622	23492	0.99954	0.99517	0.01414	0.0868	0.690	0.99061	0.99769	0.00406
0.676	23480	0.99960	0.99669	0.01467	0.0828	0.705	0.99052	0.99776	0.00428
0.735	23463	0.99961	0.99749	0.01411	0.0844	0.715	0.99048	0.99768	0.00437
0.798	23449	0.99962	0.99789	0.01299	0.0827	0.715	0.99039	0.99765	0.00421
0.856	23431	0.99967	0.99805	0.01214	0.0794	0.700	0.99077	0.99766	0.00409
0.911	23415	0.99967	0.99816	0.01191	0.0790	0.715	0.99046	0.99759	0.00434
0.969	23398	0.99972	0.99825	0.01106	0.0784	0.715	0.99058	0.99758	0.00419
1.031	23381	0.99972	0.99831	0.01084	0.0776	0.725	0.99040	0.99752	0.00438
1.097	23362	0.99971	0.99833	0.01028	0.0747	0.730	0.99044	0.99745	0.00440
1.167	23339	0.99973	0.99843	0.00935	0.0737	0.735	0.99044	0.99742	0.00442
1.241	23318	0.99974	0.99842	0.00826	0.0725	0.735	0.99043	0.99734	0.00424
1.32	23299	0.99974	0.99846	0.00715	0.0697	0.740	0.99054	0.99731	0.00431
1.405	23270	0.99977	0.99850	0.00628	0.0683	0.740	0.99046	0.99743	0.00436
1.494	23506	0.99976	0.99828	0.00613	0.0656	0.735	0.99065	0.89860	0.00428
1.589	23201	0.99979	0.99779	0.00781	0.0529	0.720	0.99120	0.99722	0.00468
1.691	23509	0.99967	0.99817	0.00491	0.0568	0.715	0.99016	0.38636	0.00434

Table 3: RHRS, E = 1.2 GeV, 2.5T 90 deg Target Field (Normal Ammonia Cell)

p0 (GeV/c)	Run #	Det Eff (Cer)	Det Eff (PR)	$(\pi/e)_{raw}$	Cut on E_1/p0	Cut on E_{tot}/p0	Cut Eff (PR)	Cut Eff (PR)	$(\pi/e)_{final}$
0.548	23886	0.99952	0.98976	0.00664	0.0876	0.675	0.99083	0.99740	0.00403
0.583	23868	0.99955	0.99291	0.00661	0.0858	0.680	0.99070	0.99731	0.00413
0.620	23858	0.99957	0.99500	0.00624	0.0871	0.675	0.99073	0.99730	0.00402
0.660	23840	0.99958	0.99619	0.00658	0.0848	0.695	0.99060	0.99723	0.00438
0.702	23826	0.99961	0.99710	0.00620	0.0855	0.680	0.99050	0.99718	0.00411
0.746	23813	0.99959	0.99739	0.00638	0.0858	0.695	0.99035	0.99717	0.00442
0.794	23792	0.99961	0.99777	0.00596	0.0831	0.685	0.99041	0.99678	0.00422
0.845	23774	0.99964	0.99785	0.00565	0.0805	0.685	0.99056	0.99666	0.00408
0.870	23946	0.99964	0.99792	0.00569	0.0805	0.685	0.99046	0.99701	0.00417
0.899	23756	0.99965	0.99792	0.00567	0.0801	0.690	0.99051	0.99664	0.00416
0.936	23934	0.99966	0.99793	0.00585	0.0791	0.685	0.99049	0.99687	0.00424
0.956	23734	0.99964	0.99795	0.00592	0.0774	0.695	0.99042	0.99671	0.00428
1.006	23906	0.99968	0.99784	0.00641	0.0736	0.690	0.99060	0.99673	0.00440
1.017	23698	0.99966	0.99763	0.00668	0.0728	0.695	0.99055	0.99682	0.00450
1.082	23895	0.99961	0.99634	0.01045	0.0665	0.615	0.99002	0.99579	0.00469
1.15	23893	0.99868	0.99509	0.00556	0.0226	0.610	0.98996	0.98845	0.00455

Table 4: RHRS, E = 1.2 GeV, 2.5T 90 deg Target Field (Short Ammonia Cell)

p0 (GeV/c)	Run #	Det Eff (Cer)	Det Eff (PR)	$(\pi/e)_{raw}$	Cut on E_1/p0	Cut on E_{tot}/p0	Cut Eff (PR)	Cut Eff (PR)	$(\pi/e)_{final}$
0.651	24095	0.99961	0.99603	0.00669	0.0860	0.690	0.99061	0.99745	0.00421
0.700	24060	0.99963	0.99687	0.00643	0.0866	0.685	0.99028	0.99736	0.00434
0.753	24025	0.99963	0.99750	0.00602	0.0850	0.675	0.99056	0.99736	0.00403
0.809	23995	0.99965	0.99773	0.00583	0.0816	0.685	0.99060	0.99719	0.00417
0.870	23974	0.99964	0.99739	0.00688	0.0805	0.685	0.98958	0.99709	0.00480

Table 5: RHRS, E = 2.2 GeV, 5T 0 deg Target Field									
p0 (GeV/c)	Run #	Det Eff (Cer)	Det Eff (PR)	$(\pi/e)_{raw}$	Cut on E_1/p0	Cut on E_{tot}/p0	Cut Eff (PR)	Cut Eff (PR)	$(\pi/e)_{final}$
0.991	24591	0.99967	0.99815	0.02719	0.0767	0.720	0.99043	0.99725	0.00434
1.055	24585	0.99970	0.99825	0.02872	0.0758	0.725	0.99042	0.99744	0.00431
1.122	24561	0.99969	0.99824	0.02961	0.0749	0.730	0.99043	0.99737	0.00425
1.194	24550	0.99971	0.99827	0.03020	0.0737	0.740	0.99022	0.99738	0.00438
1.27	24532	0.99972	0.99837	0.02927	0.0709	0.745	0.99048	0.99737	0.00438
1.351	24514	0.99976	0.99832	0.02721	0.0696	0.745	0.99042	0.99745	0.00428
1.468	24486	0.99975	0.99847	0.02308	0.0695	0.750	0.99033	0.99750	0.00425
1.596	24447	0.99985	0.99849	0.01813	0.0702	0.760	0.99002	0.99766	0.00429
1.735	24350	0.99978	0.99840	0.01252	0.0611	0.765	0.99055	0.99770	0.00436
2.05	24630	0.99984	0.99824	0.00742	0.0615	0.760	0.98998	0.99802	0.00445

Table 6: RHRS, E = 2.2 GeV, 5T 90 deg Target Field									
p0 (GeV/c)	Run #	Det Eff (Cer)	Det Eff (PR)	$(\pi/e)_{raw}$	Cut on E_1/p0	Cut on E_{tot}/p0	Cut Eff (PR)	Cut Eff (PR)	$(\pi/e)_{final}$
1.016	24726	0.99916	0.99759	0.35403	0.0807	0.700	0.99017	0.99753	0.00494
1.104	24723	0.99934	0.99773	0.29034	0.0725	0.710	0.99050	0.99755	0.00498
1.175	24720	0.99945	0.99785	0.23695	0.0698	0.720	0.99069	0.99769	0.00482
1.249	24714	0.99955	0.99802	0.18569	0.0689	0.730	0.99049	0.99790	0.00485
1.329	24708	0.99964	0.99815	0.14066	0.0662	0.735	0.99059	0.99797	0.00478
1.414	24698	0.99970	0.99828	0.10316	0.0665	0.740	0.99051	0.99811	0.00445
1.504	24691	0.99974	0.99828	0.07206	0.0638	0.755	0.99053	0.99811	0.00480
1.6	24684	0.99974	0.99835	0.05237	0.0625	0.750	0.99058	0.99798	0.00445
1.703	24677	0.99978	0.99840	0.02807	0.0599	0.760	0.99068	0.99809	0.00456
1.811	24662	0.99981	0.99845	0.01460	0.0585	0.765	0.99062	0.99815	0.00449
1.926	24648	0.99983	0.99849	0.00814	0.0571	0.770	0.99089	0.99815	0.00428
2.05	24631	0.99984	0.99827	0.00744	0.0615	0.760	0.99003	0.99808	0.00439

Table 7: RHRS, E = 3.3 GeV, 5T 90 deg Target Field									
p0 (GeV/c)	Run #	Det Eff (Cer)	Det Eff (PR)	$(\pi/e)_{raw}$	Cut on E_1/p0	Cut on E_{tot}/p0	Cut Eff (PR)	Cut Eff (PR)	$(\pi/e)_{final}$
1.945	24770	0.99950	0.99820	0.28367	0.0566	0.745	0.99056	0.99776	0.00515
2.070	24754	0.99962	0.99834	0.19549	0.0541	0.755	0.99070	0.99788	0.00512
2.202	24736	0.99971	0.99835	0.13156	0.0563	0.760	0.99078	0.99805	0.00453

5.2 Left HRS Results

Note that for all kinematic settings, the cut on the gas Cherenkov is at channel 200.

Table 8: LHRS, E = 2.2 GeV, 2.5T 90 deg Target Field									
p0 (GeV/c)	Run #	Det Eff (Cer)	Det Eff (PR)	$(\pi/e)_{raw}$	Cut on $E_1/p0$	Cut on $E_{tot}/p0$	Cut Eff (PR)	Cut Eff (PR)	$(\pi/e)_{final}$
0.541	3935	0.99968	0.98105	0.05227	0.255	0.580	0.98976	0.99914	0.00442
0.582	3929	0.99970	0.98746	0.04898	0.254	0.580	0.98976	0.99911	0.00431
0.626	3922	0.99974	0.99171	0.04589	0.252	0.585	0.98973	0.99920	0.00445
0.673	3915	0.99973	0.99445	0.04272	0.253	0.585	0.98972	0.99923	0.00435
0.724	3907	0.99978	0.99322	0.04049	0.251	0.590	0.98970	0.99932	0.00445
0.778	3901	0.99978	0.99593	0.03760	0.244	0.590	0.98970	0.99935	0.00443
0.837	3893	0.99984	0.99757	0.03564	0.246	0.590	0.98971	0.99940	0.00430
0.900	3885	0.99981	0.99841	0.03474	0.244	0.595	0.98967	0.99935	0.00450
0.968	3882	0.99988	0.99888	0.03381	0.240	0.595	0.98961	0.99943	0.00446
1.003	3643	0.99992	0.99901	0.03434	0.237	0.595	0.98961	0.99938	0.00448
1.041	3872	0.99986	0.99915	0.03314	0.238	0.595	0.98981	0.99943	0.00436
1.078	3628	0.99995	0.99928	0.03371	0.239	0.595	0.98971	0.99945	0.00429
1.119	3866	0.99989	0.99931	0.03217	0.238	0.595	0.98978	0.99946	0.00424
1.159	3616	0.99994	0.99938	0.03302	0.236	0.600	0.98962	0.99941	0.00447
1.203	3845	0.99989	0.99940	0.03142	0.233	0.595	0.98975	0.99948	0.00436
1.247	3596	0.99994	0.99943	0.03085	0.231	0.595	0.98971	0.99946	0.00431
1.294	3834	0.99991	0.99947	0.02941	0.229	0.595	0.98987	0.99946	0.00434
1.340	3585	0.99995	0.99952	0.02811	0.227	0.590	0.99019	0.99941	0.00398
1.391	3823	0.99990	0.99948	0.02700	0.226	0.595	0.98960	0.99943	0.00445
1.441	3554	0.99995	0.99957	0.02576	0.226	0.595	0.98970	0.99946	0.00434
1.496	3817	0.99993	0.99951	0.02333	0.221	0.590	0.99001	0.99948	0.00428
1.550	3531	0.99996	0.99959	0.02176	0.223	0.595	0.98978	0.99940	0.00442
1.608	3787	0.99992	0.99957	0.01957	0.219	0.590	0.98989	0.99945	0.00422
1.667	3520	0.99997	0.99956	0.01764	0.218	0.590	0.98986	0.99946	0.00425
1.729	3774	0.99992	0.99954	0.01550	0.219	0.590	0.98977	0.99945	0.00427
1.792	3497	0.99996	0.99959	0.01365	0.218	0.590	0.98979	0.99951	0.00428
1.859	3772	0.99992	0.99960	0.01175	0.216	0.590	0.98977	0.99934	0.00436
1.927	3477	0.99996	0.99969	0.01005	0.215	0.585	0.99015	0.99948	0.00397
1.940	3941	0.99993	0.99962	0.01018	0.212	0.585	0.98985	0.99946	0.00423
2.072	3457	0.99997	0.99902	0.01118	0.197	0.575	0.98989	0.99937	0.00418
2.228	3444	0.99996	0.99980	0.00871	0.212	0.590	0.99002	0.99941	0.00413

Table 9: LHRS, E = 1.7 GeV, 2.5T 90 deg Target Field									
p0 (GeV/c)	Run #	Det Eff (Cer)	Det Eff (PR)	$(\pi/e)_{raw}$	Cut on E_1/p0	Cut on E_{tot}/p0	Cut Eff (PR)	Cut Eff (PR)	$(\pi/e)_{final}$
0.572	4551	0.99976	0.98683	0.02347	0.255	0.585	0.98965	0.99926	0.00447
0.622	4539	0.99976	0.99159	0.02125	0.254	0.585	0.98949	0.99928	0.00448
0.676	4528	0.99982	0.99472	0.01964	0.254	0.590	0.98957	0.99929	0.00451
0.735	4513	0.99984	0.99402	0.01796	0.250	0.590	0.98973	0.99936	0.00447
0.798	4496	0.99983	0.99667	0.01664	0.251	0.590	0.98974	0.99938	0.00425
0.856	4482	0.99987	0.99785	0.01574	0.255	0.590	0.98960	0.99937	0.00404
0.911	4465	0.99987	0.99848	0.01553	0.244	0.595	0.98964	0.99940	0.00437
0.969	4445	0.99987	0.99894	0.01448	0.244	0.590	0.99006	0.99944	0.00401
1.031	4428	0.99989	0.99910	0.01446	0.241	0.595	0.98971	0.99945	0.00427
1.097	4409	0.99990	0.99925	0.01374	0.239	0.595	0.98981	0.99944	0.00425
1.167	4384	0.99989	0.99932	0.01368	0.233	0.600	0.98960	0.99942	0.00456
1.241	4358	0.99990	0.99938	0.01219	0.234	0.595	0.98970	0.99945	0.00421
1.32	4341	0.99989	0.99939	0.01100	0.230	0.595	0.98964	0.99941	0.00429
1.405	4292	0.99989	0.99948	0.00978	0.229	0.595	0.98997	0.99941	0.00414
1.494	4332	0.99991	0.99943	0.01002	0.220	0.605	0.98922	0.99940	0.00433
1.589	4220	0.99992	0.99892	0.01139	0.214	0.590	0.98934	0.99929	0.00446
1.691	4574	0.99990	0.99979	0.00867	0.231	0.605	0.98997	0.99915	0.00403

Table 10: LHRS, E = 1.2 GeV, 2.5T 90 deg Target Field (Normal Ammonia Cell)									
p0 (GeV/c)	Run #	Det Eff (Cer)	Det Eff (PR)	$(\pi/e)_{raw}$	Cut on E_1/p0	Cut on E_{tot}/p0	Cut Eff (PR)	Cut Eff (PR)	$(\pi/e)_{final}$
0.548	5007	0.99975	0.98134	0.01099	0.252	0.575	0.98997	0.99917	0.00438
0.583	4987	0.99979	0.98667	0.01075	0.257	0.580	0.98982	0.99916	0.00446
0.620	4980	0.99981	0.99060	0.01035	0.255	0.580	0.98973	0.99922	0.00439
0.660	4963	0.99983	0.99377	0.00974	0.252	0.580	0.98974	0.99922	0.00423
0.702	4949	0.99984	0.99146	0.00985	0.254	0.585	0.98967	0.99923	0.00433
0.746	4931	0.99986	0.99464	0.00961	0.247	0.585	0.98952	0.99922	0.00432
0.794	4905	0.99986	0.99641	0.00993	0.247	0.595	0.98937	0.99918	0.00469
0.845	4886	0.99986	0.99741	0.00943	0.246	0.590	0.98961	0.99920	0.00434
0.870	5089	0.99986	0.99781	0.00858	0.237	0.575	0.99017	0.99921	0.00392
0.896	4861	0.99986	0.99814	0.00968	0.245	0.595	0.98933	0.99910	0.00445
0.936	5070	0.99986	0.99842	0.00968	0.239	0.590	0.98946	0.99920	0.00443
0.956	4841	0.99986	0.99860	0.00988	0.241	0.595	0.98941	0.99918	0.00453
1.006	5047	0.99986	0.99875	0.01019	0.233	0.590	0.98951	0.99916	0.00446
1.017	4788	0.99988	0.99787	0.01261	0.222	0.585	0.98830	0.99892	0.00487
1.082	5034	0.99976	0.99762	0.01580	0.207	0.580	0.98864	0.99843	0.00500
1.113	5030	0.99934	0.99903	0.00945	0.228	0.575	0.98998	0.99467	0.00415
1.150	5029	0.99983	0.99855	0.00952	0.216	0.570	0.98612	0.98624	0.00404
1.168	5025	0.99870	0.99834	0.00944	0.214	0.590	0.98997	0.99236	0.00395

Table 11: LHRS, E = 1.2 GeV, 2.5T 90 deg Target Field (Short Ammonia Cell)

p0 (GeV/c)	Run #	Det Eff (Cer)	Det Eff (PR)	$(\pi/e)_{raw}$	Cut on E_1/p0	Cut on E_{tot}/p0	Cut Eff (PR)	Cut Eff (PR)	$(\pi/e)_{final}$
0.523	5290	0.99980	0.97312	0.01211	0.252	0.565	0.98971	0.99924	0.00423
0.563	5288	0.99980	0.98199	0.01097	0.249	0.565	0.98989	0.99927	0.00422
0.651	5265	0.99985	0.99231	0.01033	0.249	0.575	0.98965	0.99937	0.00437
0.700	5238	0.99985	0.99474	0.01011	0.249	0.580	0.98941	0.99930	0.00451
0.746	5322	0.99988	0.99398	0.00942	0.244	0.575	0.98998	0.99935	0.00418
0.753	5200	0.99985	0.99442	0.00973	0.244	0.580	0.98980	0.99936	0.00444
0.794	5320	0.99984	0.99620	0.00910	0.242	0.575	0.99004	0.99926	0.00416
0.845	5318	0.99983	0.99733	0.00881	0.241	0.575	0.99010	0.99934	0.00404
0.870	5138	0.99987	0.99689	0.01120	0.228	0.575	0.98883	0.99924	0.00469
0.896	5316	0.99982	0.99821	0.00909	0.240	0.580	0.99009	0.99932	0.00426
0.956	5276	0.99985	0.99867	0.00911	0.234	0.585	0.98983	0.99932	0.00426
1.017	5274	0.99990	0.99847	0.00986	0.212	0.570	0.99008	0.99927	0.00415
1.082	5272	0.99985	0.99698	0.01435	0.170	0.540	0.99001	0.99895	0.00453

Table 12: LHRS, E = 2.2 GeV, 5T 0 deg Target Field

p0 (GeV/c)	Run #	Det Eff (Cer)	Det Eff (PR)	$(\pi/e)_{raw}$	Cut on E_1/p0	Cut on E_{tot}/p0	Cut Eff (PR)	Cut Eff (PR)	$(\pi/e)_{final}$
0.991	5902	0.99989	0.99890	0.02800	0.244	0.595	0.98963	0.99938	0.00436
1.055	5890	0.99987	0.99915	0.02914	0.241	0.595	0.98987	0.99933	0.00430
1.122	5885	0.99987	0.99929	0.02926	0.239	0.590	0.98992	0.99938	0.00403
1.194	5872	0.99989	0.99933	0.02996	0.236	0.595	0.98982	0.99941	0.00435
1.27	5866	0.99988	0.99939	0.02907	0.233	0.590	0.98990	0.99938	0.00421
1.351	5855	0.99990	0.99943	0.02766	0.231	0.590	0.98975	0.99944	0.00420
1.468	5838	0.99991	0.99950	0.02453	0.228	0.590	0.98972	0.99946	0.00431
1.596	5829	0.99992	0.99951	0.01999	0.223	0.585	0.98991	0.99948	0.00419
1.735	5827	0.99993	0.99953	0.01499	0.219	0.580	0.99003	0.99949	0.00402
1.886	5781	0.99996	0.99964	0.01079	0.213	0.580	0.99010	0.99954	0.00416
2.05	5706	0.99992	0.99924	0.01046	0.205	0.575	0.98989	0.99942	0.00417
2.228	5630	0.99992	0.99986	0.00836	0.215	0.585	0.99014	0.99934	0.00397

Table 13: LHRS, E = 2.2 GeV, 5T 90 deg Target Field

p0 (GeV/c)	Run #	Det Eff (Cer)	Det Eff (PR)	$(\pi/e)_{raw}$	Cut on E_1/p0	Cut on E_{tot}/p0	Cut Eff (PR)	Cut Eff (PR)	$(\pi/e)_{final}$
0.919	6085	0.99921	0.99822	0.46241	0.239	0.600	0.98972	0.99875	0.00454
1.016	6084	0.99943	0.99865	0.37722	0.230	0.600	0.98960	0.99899	0.00458
1.104	6083	0.99966	0.99891	0.30164	0.230	0.605	0.98962	0.99927	0.00475
1.175	6059	0.99968	0.99909	0.24180	0.231	0.600	0.98964	0.99933	0.00444
1.249	6053	0.99976	0.99917	0.19667	0.227	0.605	0.98951	0.99938	0.00470
1.329	6044	0.99978	0.99925	0.15003	0.227	0.605	0.98941	0.99941	0.00465
1.414	6031	0.99984	0.99934	0.11008	0.228	0.605	0.98945	0.99949	0.00468
1.504	6021	0.99990	0.99941	0.07824	0.222	0.605	0.98928	0.99955	0.00479
1.6	6011	0.99988	0.99940	0.05755	0.219	0.590	0.98999	0.99952	0.00405
1.703	6002	0.99990	0.99947	0.03308	0.216	0.600	0.98949	0.99953	0.00459
1.811	5978	0.99992	0.99958	0.01885	0.216	0.600	0.98948	0.99957	0.00451
1.926	5962	0.99994	0.99961	0.01181	0.213	0.595	0.98988	0.99958	0.00419
2.05	5954	0.99994	0.99925	0.01052	0.199	0.585	0.99003	0.99954	0.00417
2.228	6065	0.99994	0.99988	0.00804	0.208	0.595	0.99017	0.99966	0.00401

Table 14: LHRS, E = 3.3 GeV, 5T 90 deg Target Field									
p0 (GeV/c)	Run #	Det Eff (Cer)	Det Eff (PR)	$(\pi/e)_{raw}$	Cut on E_1/p0	Cut on E_{tot}/p0	Cut Eff (PR)	Cut Eff (PR)	$(\pi/e)_{final}$
2.342	6148	0.99990	0.99952	0.08573	0.200	0.585	0.98980	0.99952	0.00427
2.492	6157	0.99991	0.99959	0.05089	0.197	0.585	0.98975	0.99955	0.00438
2.651	6170	0.99993	0.99960	0.02928	0.195	0.580	0.98995	0.99604	0.00408
2.800	6183	0.99995	0.99960	0.01720	0.191	0.580	0.98972	0.99955	0.00433
2.820	6129	0.99996	0.99960	0.01589	0.189	0.580	0.98978	0.99951	0.00433
3.000	6207	0.99996	0.99961	0.01068	0.185	0.575	0.98998	0.99962	0.00420

References

[1] J. Alcorn et al. *Basic Instrumentation for Hall A at Jefferson Lab*, Nuclear Instruments and Methods, A522, 294-346 (2004).

[2] H.J. Lu et al. *Shower Calibration & Efficiency for E97-110*. E97110 Technical note (2005).

[3] K. Slifer. *Shower Detector Calibration and Cut Optimization for E94010*. E94010 Technical note (2000).